Star Formation Rate of the Low Redshift Dwarf Galaxies J080947.50+213717.2 and J151839.94+220514.4

S. P. Gautam, A. Silwal, A. Sedain, B. Aryal

Journal of Nepal Physical Society

Volume 7, Issue 1, April 2021

(Special Issue: ANPA Conference, 2020)

ISSN: 2392-473X (Print), 2738-9537 (Online)

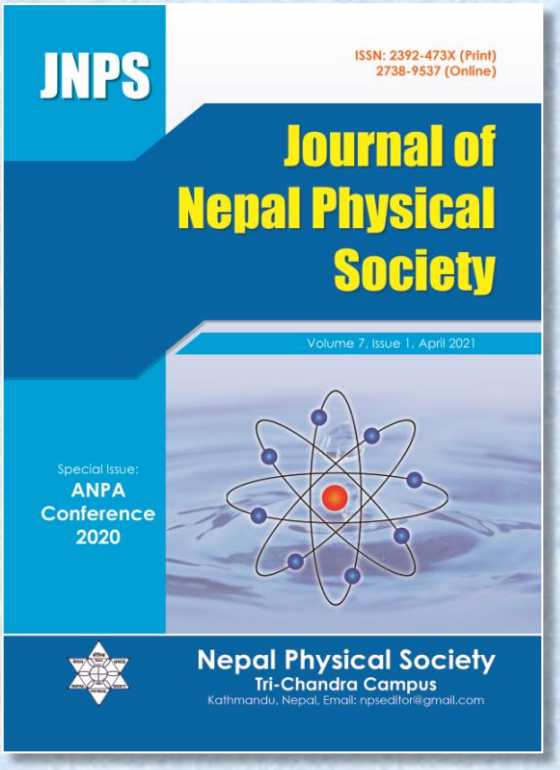

Editors:

Dr. Santosh KC

San Jose State University, USA (Editor in Chief)

Dr. Pashupati Dhakal

Thomas Jefferson National Accelerator Facility, USA

Dr. Yadav Pandit

Baptist Health Science University, USA

Managing Editor:

Dr. Binod Adhikari

St. Xavier's College, Kathmandu, Nepal

JNPS, **7** (1), 18-24 (2021)

DOI: http://doi.org/10.3126/jnphyssoc.v7i1.36969

Published by:

Nepal Physical Society

P.O. Box: 2934

Tri-Chandra Campus

Kathmandu, Nepal

Email: npseditor@gmail.com

JNPS 7 (1): 18-24 (2021)
ISSN: 2392-473X (Print), 2738-9537 (Online)
Research Article *© Nepal Physical Society*
DOI: http://doi.org/10.3126/jnphyssoc.v7i1.36969

Star Formation Rate of the Low Redshift Dwarf Galaxies J080947.50+213717.2 and J151839.94+220514.4

S. P. Gautam[1*], A. Silwal[2], A. Sedain[1], B. Aryal[1]
[1]Central Department of Physics, Tribhuvan University, Kirtipur, Nepal
[2]Patan Multiple Campus, Tribhuvan University, Lalitpur, Nepal
[*]Corresponding Email: astrosujan@gmail.com

Received: *9 August, 2020;* ***Revised:*** *26 January, 2021;* ***Accepted:*** *8 February, 2021*

ABSTRACT

We performed a spectroscopic analysis of two low redshift dwarf galaxies, SDSSJ080947.50+213717.2, and SDSSJ151839.94+220514.4 selected from a catalogue of Paudel et al. 2018. The strong emission lines of the SDSS spectra of both galaxies were studied and the elements responsible were identified for those characteristic lines. The line ratio between Hα and Hβ (Hα/Hβ) for the galaxies SDSSJ080947.50+213717.2 and SDSSJ151839.94+220514.4 was found to be 2.77 and 2.75, respectively, suggesting these are nearly dust free and star forming galaxies. The star formation rate of the galaxies SDSSJ080947.50+213717.2 and SDSSJ151839.94+220514.4 was found to be 0.0232 $M_{\odot}yr^{-1}$ and 0.05221 $M_{\odot}yr^{-1}$, respectively. The ratio between NII and Hα was used to calculate the emission line metallicity, which was found to be 8.13 dex and 8.46 dex for the galaxies SDSSJ080947.50+213717.2 and SDSSJ151839.94+220514.4, respectively. From the comparison of our findings with the previous studies, slightly lower star formation rate than normal galaxies were noticed. The metallicity value for both of the galaxies were positioned in the group of low-surface-brightness galaxies of Bargvell's dwarfs.

Keywords: Star Formation Rate, SDSS, Dwarf Galaxy, Spectroscopy

1. INTRODUCTION

Low-luminosity, dwarf galaxies are the most common types of galaxies in the universe [1]. They have a small size, small absolute luminosity, low surface brightness, and relatively low mass ~10^8 $M_{\odot}$ [2]. Determination of star formation history and possible predictions for future star births is one of the important problems in extragalactic astronomy [3]. The physics of star formation is very complicated to understand and apply in the models of galaxy formation and evolution, so the first natural step is to find constraints from the observational studies by evaluating an infallible star formation rate (SFR) at several scales and redshifts, and obtaining the key derivers of its variations [4].

Past studies of SFR generally concerned bright and rapidly star-forming galaxies, however recent works (James *et al.*, Kennicutt et al.) [5, 6] have performed the measurement of SFR for a full range of galaxy types and brightness. Due to low luminosities, a small amount of data for internal extinction, and heavier elements abundances, dwarf and irregular galaxies are the biggest challenges. Although there are many other techniques (e.g., ultraviolet emission from stars, far-infrared and radio luminosities), Hα observations are the easiest commonly used method for SFR estimations. Lee et al. [7] found a galaxy's UV flux probes a fuller mass spectrum of massive stars, and thus measures star formation averaged over a longer ~ 108 yr time-scale. However, UV emission alone is not sufficient tracer of the SFR. Hα and UV SFRs for nearby galaxies have been compared by several authors (e.g. Salim et al. and references therein) [8], UV SFRs are noticed to be slightly lower than Hα SFRs. This finding is also supported by the results of Lee et al. [7], in which they estimated the ratio of Hα SFRs to the UV SFRs in the range 0.26 to 1.16. The difference is caused due to the effects of internal dust extinction which lowers the observed UV flux. Due to difference in

the dust attenuation evaluation, these two methods of SFR calculation are altered from perfect agreement [7]. Galaxies with weak or no Hα emission, UV measurement is extremely useful for the estimation of reliable SFR [7].

Metallicity indirectly draws star formation history that demonstrates the balance of many crucial physical mechanisms of the galaxies such as ejection of metals into the ISM through supernova and stellar winds, the expulsions of the gas via galactic outflows, and the accumulation of gas on the galaxy from the local environments [9]. The physical mechanism that regulates star formation and importantly, galaxy evolution can be understood analyzing evolution of metallicity in relation to the other essential galaxy properties [9]. Andjelic [3] determined the star formation rate using Hα fluxes for dwarf galaxy Holmberg IX, which was found to be 3.4×10^{-4} $M_{\odot}yr^{-1}$. Chhatkuli et al. [10] calculated the star formation rate of low redshift (z = 0.00837) dwarf galaxy, which was found to be 0.019 $M_{\odot}yr^{-1}$, with Hα/Hβ = 2.73 and emission line metallicity, 12 + log(O/H) = 7.85 dex.

In this paper, we performed a SDSS spectroscopic analysis of two dwarf galaxies, selected from the catalogue of Paudel et al. [11], to estimate the star formation rate and emission line metallicity. The paper is organized as follows. In Sect. 2, we lay out our methods. We present our results and discussion in Sect.3, and we conclude our study in Sect. 4.

2. METHODS

A catalogue of merging dwarf galaxies in the local universe, prepared by Paudel et al., 2018 includes 177 nearby merging dwarf galaxies of stellar mass $M_{*} < 10^{10}$ $M_{\odot}$ and redshifts z < 0.02. We selected two interesting tidal tail featured dwarf galaxies, shown in Table 2.1, SDSSJ080947.50+213717.2 (R.A.: 08h 09m 47.50s & Dec.: 21d 37m 17.2s) and SDSSJ151839.94+220514.4 (R.A.: 15h 18m 39.94s & Dec.:22d 05m 14.4s) with redshift values 0.0111 and 0.0158, respectively. SDSS (Sloan Digital Sky Survey) released fourth data from the fourth phase of the survey at different bands with exposure time per band: 53.9 seconds. We downloaded the SDSS DR16 sky flux subtracted spectral data of these galaxies from SDSS server (http://skyserver.sdss.org/dr16), for this, coordinates and redshift values given in the catalog was used. After downloading spectra data, we identified the characteristic peaks of emission lines of the spectra and plotted them using the software ORIGIN8.5. We performed the Gaussian fit on the data points and obtained the statistical parameters such as full width half maximum (FWHM), area, Gaussian center, regression coefficient, height of the Gaussian, offset of the characteristic lines. For the estimation of SFR of these galaxies, we adopted the techniques of Hα measurement suggested by Kennicutt, 1998 [12]. The star formation rate from the Hα measurement can be estimated as,

$$SFR\ (M_{\odot}yr^{-1}) = 7.94\ \times\ 10^{-42} \sum L_{H\alpha}\ (ergs^{-1}) \quad (1)$$

$$SFR\ (M_{\odot}yr^{-1}) = 7.94\ \times 10^{-42}\ \times \text{Area of Gaussian fit}\ \times\ 10^{-17}\ \times 4\pi R^{2} \quad (2)$$

Where, $R = D \times 3.08 \times 10^{24}$ cm, D is the distance to the galaxy. SFR is given in solar masses per year, and $L_{H\alpha}$ is Hα luminosity of the galaxy. This transformation is appropriate under the assumption of average solar abundances and Salpeter initial mass function (Salpeter 1955), for a range of stellar masses from 0.1−100 $M_{\odot}$[3].

Emission line metallicity was estimated by using a line ratio between Hα and [NII]. Calibration provided by Marino *et al.* [13] was used.

$$12\ +\ log\ (O/H)\ =\ 8.743\ +\ 0.462\ \times\ log\ (NII/\ H\alpha) \quad (3)$$

Table 2.1: Data for the dwarf galaxies selected from the catalogue of Paudel et al., 2018 [11].

ID	RA (deg)	DEC(deg)	z	m_g (mag)	m_r (mag)	m_{FUV}	m_{NUV}	Feature
Id08092137	122.4474	21.6215	0.0111	15.98	15.75	16.42	15.34	T
Id15182205	229.6666	22.0863	0.0158	15.50	15.11	17.09	17.47	T

**In the above table, T-feature represents the tidal tail featured dwarf galaxy which is categorized in the catalog list on the basis of morphologies [11] of the galaxies.*

3. RESULTS AND DISCUSSION

3.1 Dwarf Galaxy: J080947.50+213717.2

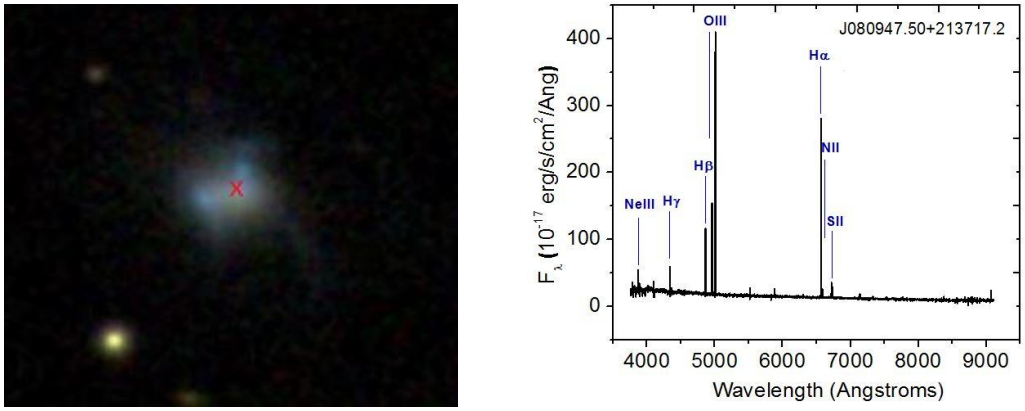

Fig. 3.1: Optical view (left) [image: SDSS DR16 server], and SDSS spectrum (right), of the dwarf galaxy SDSSJ080947.50+213717.2.

Optical view and SDSS spectrum of the galaxy SDSSJ080947.50+213717.2 is shown in the Figure 3.1. '×' symbol represents the central position of the galaxy. The wavelength ranges from 3757 to 9210 Å, whereas intensity goes from 1.6 to 409.6 erg $s^{-1}cm^{-2}$ $Å^{-1}$. Although some absorption features are also seen, these spectra are mostly dominated by the emission mechanism. We performed a Gaussian fit of all the characteristic emission of a spectrum lines, the corrected value of intensities of each peak with respect to best fit in the continuum was calculated. Similarly, the peak wavelengths were corrected using the redshift of the galaxies.

Table 3.1: Statistical parameters estimated from the Gaussian fit of characteristic emissions from the spectra of the galaxy SDSSJ080947.50+213717.2.

peaks	Gaussian peak (Å)	Wavelength peak (Å)	I(peak) ($\times10^{-17}$ erg/s/cm^2/Å)	Offset (Å)	FWHM (Å)	Area ($\times10^{-17}$ erg/s/cm^2/Å)	R^2	Emissions
1	5008.13	5008.47 ± 0.02	416.69 ± 4.12	0.34	2.82	1279.31 ±45.95	0.99	OIII
2	4960.26	4960.27 ± 0.01	138.03 ± 1.33	0.01	2.87	430.23 ± 9.57	0.99	OIII
3	4862.59	4863.01 ± 0.01	101.12 ± 0.76	0.42	2.64	307.95 ± 5.94	0.99	Hβ
4	4341.59	4341.16 ± 0.04	47.42 ± 1.96	-0.43	2.77	148.6 ± 12.99	0.98	Hγ
5	3869.46	3869.48 ± 0.05	34.47 ± 1.25	0.02	3.02	109.35 ± 9.30	0.98	NeIII
6	6564.67	6564.56 ± 0.02	280.51 ± 2.75	-0.11	3.95	1152.5 ± 30.32	0.99	Hα
7	6718.59	6719.01 ± 0.03	23.15 ± 0.44	0.42	4.03	100.29 ± 4.39	0.99	SII
8	6732.97	6732.95 ± 0.07	16.35 ± 0.63	-0.02	3.84	68.37 ± 6.12	0.99	SII
9	6585.76	6585.35 ± 0.06	13.38 ± 0.82	-0.41	3.35	51.24 ± 4.68	0.98	NII

We analyzed the nine main emission lines, i.e., [OIII], Hβ, Hγ, [NeIII], Hα, [SII], which are identified in Fig. 3.1 (right). We found [OIII] and [SII] are doublets, so they have two different emission lines. The characteristic emissions of the galaxy show nearly perfect Gaussian nature with a regression coefficient of more than 98%. The intensity and area of the Hα were found to be 280.51×10^{-17} erg/s/cm^2/Å and 1152.2×10^{-17} erg/s/cm^2/Å, respectively. The maximum intensity, 416.69×10^{-17} erg/s/cm^2/Å, was obtained for

the doubly ionized oxygen [OIII]. The minimum intensity among nine emission lines was found to be 13.38 erg/s/cm^2/Å for [NII]. The value of full with half maximum was less than 4.03 Å for all the emissions. The statistical parameters obtained from the Gaussian fit are listed in Table 3.1.

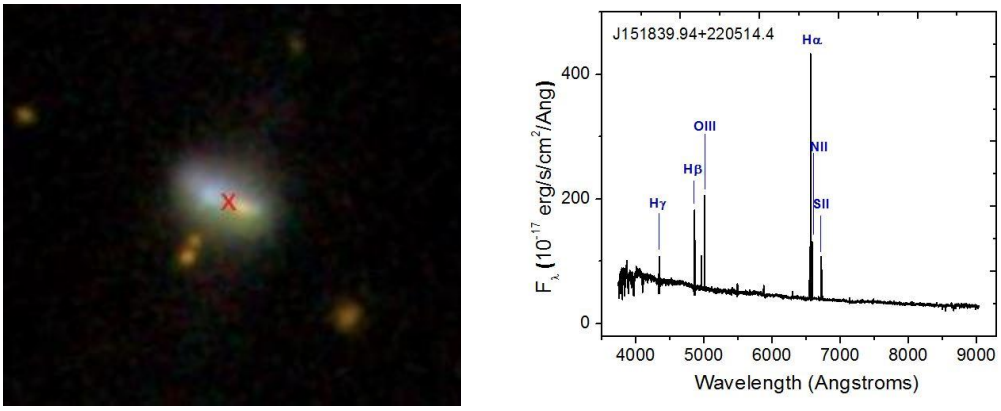

Fig. 3.2: Optical view (left) [image: SDSS DR16 server], and SDSS spectrum (right), of the dwarf galaxy SDSSJ151839.94+220514.4.

The star formation rate of the selected dwarf galaxy was calculated using Eq. (2). Hubble's distance D of the galaxies was calculated by using Hubble's law for a given redshift. The star formation rate in this galaxy was found to be 0.02321 $M_\odot yr^{-1}$. The presence of internal dust reddening can be estimated using the line ratio between Hα and Hβ [10], due to its usefulness in the future studies, line ratio between Hα and Hβ was also estimated. The line ratio of Hα and Hβ (Hα/Hβ) of the galaxy was measured to be 2.77, which is slightly lower than the theoretical value (i.e., Hα/Hβ = 2.8 for star forming galaxies as estimated by Dessauges-Zavadsky et al. [14]). This indicates that this galaxy shows the nature of star forming galaxies. The emission lines metallicity for this galaxy was calculated using Eq. (3). Emission lines metallicity, [12 + log(O/H)] = 8.13 dex was obtained.

3.2 Dwarf Galaxy: J151839.94+220514.4

The optical view and SDSS spectrum of the galaxy SDSSJ151839.94+220514.4 is shown in Fig. 3.2. '×' symbol represents the central position of the galaxy. The wavelength ranges from 3747 to 9036 Å, whereas intensity lines in the range 20.3 to 432.7 erg $s^{-1}cm^{-2}$ $Å^{-1}$. This spectra are also mostly dominated by the emission lines. Following the similar process as previous, we performed a Gaussian fit of all the characteristic emissions of the spectra. Wavelength of the peaks was also corrected using the redshift value and the peak intensity of the emission lines for this galaxy was measured.

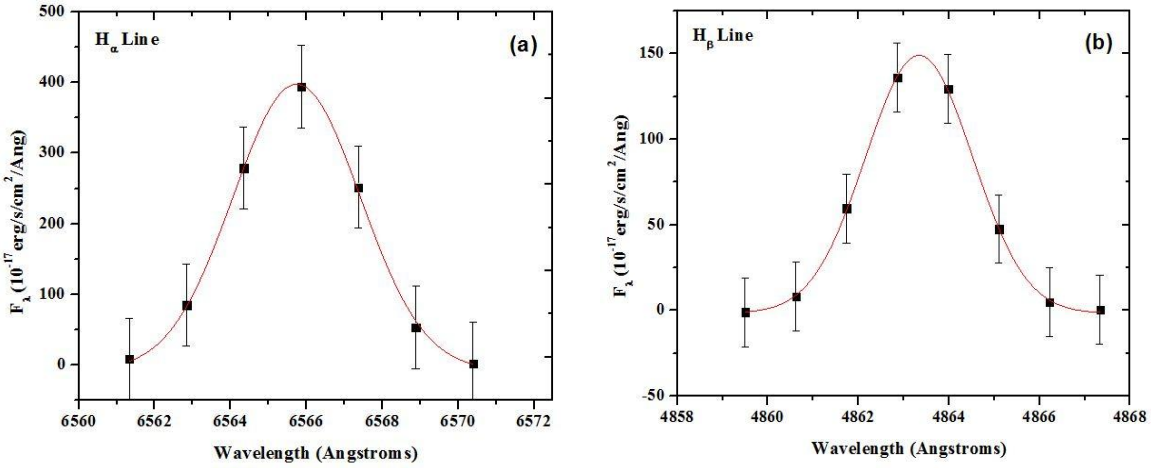

Fig. 3.3: Example of Gaussian fitting: (a) Hα line and (b) Hβ line of the spectrum of the galaxy SDSSJ151839.94+220514.4

Table 3.2: Statistical parameters obtained from the Gaussian fit of characteristic emission from the spectra of the galaxy SDSSJ151839.94+220514.4.

Peaks	Gaussian peak (Å)	Wavelength peak (Å)	I(peak) ($\times 10^{-17}$ erg/s/cm^2/Å)	Offset (Å)	FWHM (Å)	Area ($\times 10^{-17}$ erg/s/cm^2/Å)	R^2	Emissions
1	6565.74	6565.86 ± 0.02	397.26 ± 6.33	0.12	3.95	1701.68 ± 61.55	0.99	Hα
2	6586.31	6587.06 ± 0.03	100.59 ± 1.62	0.75	3.99	437.78 ± 15.91	0.99	NII
3	6550.93	6550.76 ± 0.04	31.17 ± 0.72	-0.17	4.00	135.16 ± 7.10	0.99	NII
4	6719.41	6718.8 ± 0.02	73.6 ± 0.58	-0.61	3.78	295.44 ± 6.02	0.99	SII
5	6733.8	6733.86 ± 0.06	49.08 ± 1.72	0.06	4.19	226.01 ± 17.46	0.99	SII
6	5008.99	5009.46 ± 0.01	161.9 ± 1.32	0.47	3.00	521.28 ± 11.12	0.99	OIII
7	4961.03	4961.25 ± 0.04	53.63 ± 1.27	0.22	2.84	162.94 ± 9.76	0.99	OIII
8	4863.34	4862.86 ± 0.01	144.97 ± 0.90	-0.48	2.77	445.45 ± 6.76	0.99	Hβ
9	4342.21	4342.02 ± 0.08	58.36 ± 1.17	-0.19	2.56	160.06 ± 7.97	0.99	Hγ

For this galaxy, we performed the analysis of nine main emission lines, i.e., Hα, [NII], [SII], [OIII], Hβ, Hγ, which are identified from Fig. 3.2 (right). We found [NII], [SII] and [OII] are doublets with two emission lines. The maximum intensity was found to be 397.26×10^{-17} erg/s/cm^2/Å for Hα with area 1701.68×10^{-17} erg/s/cm^2/Å. The minimum intensity, 31.17×10^{-17} erg/s/cm^2/Å, was obtained for [NII]. The characteristic emission of this galaxy was also found to show nearly perfect Gaussian nature with the value of regression coefficient more than 98%. For all the emission lines, the value of FWHM was less than 4.19 Å. The statistical parameters obtained from the Gaussian fit of emission lines are listed in Table 3.2. The star formation rate in this galaxy was found to be 0.05221 $M_{\odot}yr^{-1}$. The line ratio of Hα and Hβ (Hα/Hβ) of the galaxy was calculated as 2.75, which is also slightly lower than theoretical value (i.e., Hα/Hβ = 2.8 for SFGs [14]). The emission line meallicity of this galaxy, 12 + log(O/H), was found to be 8.46 dex for this galaxy.

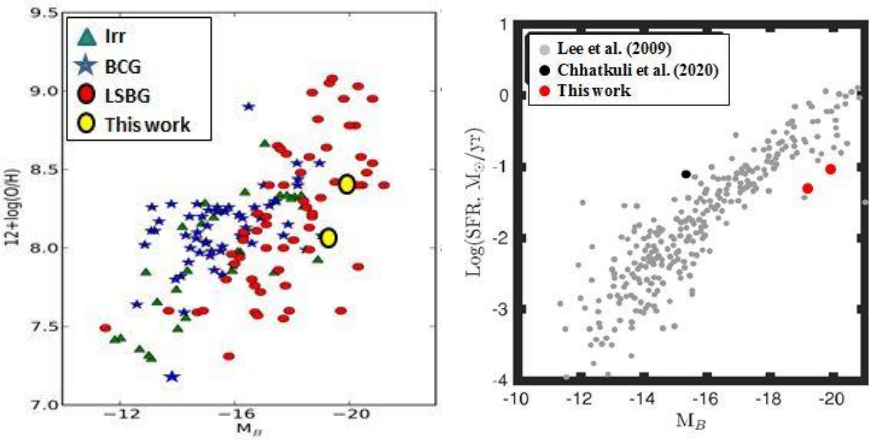

Fig. 3.4: Comparison of SFR of the present work with the previous findings (right) [Image source: Chhatkuli et al. [10]] & comparison of emission line metallicity with previous findings (left) [Image source: Bergvall [15]].

A large number of studies regarding star formation rate of the dwarf galaxies had performed in the past by different researchers. Normal galaxies obey scaling relations of B-band absolute magnitude (M_B) versus star formation rate, and M_B versus emission-line metallicity [10]. We became interested to compare our results of star formation rate with the findings of Lee et al. [16] and Chhatkuli et al. [10]. The emission line metallicity obtained for the selected dwarf galaxies were

compared with the findings of Bergvall [15]. Figure 3.4 (right) shows the M_B - SFR relationship of the dwarf galaxies. Red circle in the figure represent our galaxy sources. The star formation rate of our galaxies were found to be lower than the normal galaxies. Figure 3.4 (left) represents the M_B - emission line metallicity relation presented by Bergvall [15]. Green triangle in the figure shows the metallicty of irregular (Irr) dwarf galaxies, blue star represents the blue compact dwarf galaxies (BCG), and red circle indicates the low-surface-brightness (LSGB) dwarf galaxies. Our galaxy situated in between the group of LSGB. Objects falling under the flag of galaxies of low surface brightness tend to be forming much more slowly and even at an early stage of development than regular galaxies [17, 18]. At lower densities, they appear to be more isolated and contain more gas than what is normally contained in regular galaxies, and this low gas density is thought to obstruct the creation of massive stars [18, 19]. Since the production plants for heavy elements are massive stars, galaxies with low surface brightness have much lower metallicity than regular galaxies, that is an another indication of the slow creation of these objects [19, 20].

4. CONCLUSIONS

The strong emission line spectra of low redshift dwarf galaxies SDSSJ080947.50+213717.2 and SDSSJ151839.94+220514.4 were studied. In addition, a Gaussian model fit of the characteristic emissions was performed. The following results were obtained from the study,

- The star formation rate of the galaxies SDSSJ080947.50+213717.2 and SDSSJ151839.94+220514.4 was found to be 0.02321 $M_{\odot}yr^{-1}$ and 0.05221 $M_{\odot}yr^{-1}$ respectively.
- The line ratio, Hα/Hβ, was found to be 2.77 for SDSSJ080947.50+213717.2 and 2.75 for SDSSJ151839.94+220514.4, which were slightly lower than theoretical value (i.e. Hα/Hβ = 2.8), suggesting star forming galaxies.
- The emission lines metallicity, 12 + log(O/H), was found to be 8.13 dex for SDSSJ080947.50+213717.2 and 8.46 dex for SDSSJ151839.94+220514.4.
- From the comparison of SFR and emission-line metallicity with the previous findings, SFR of our sources were found to be slightly lower than normal galaxies. M_B - metallicty relation showed that our galaxies follows the nature of low surface brightness dwarf galaxies.

This work presented the star formation rate and the emission-line metallicity of two low redshift ($z < 0.02$) dwarf galaxies using Hα measurement. SFR using UV measurement and its comparison with the current work will be performed in the future. In addition, by conducting photometric analysis, other physical and morphological properties of the dwarf galaxies will be estimated and analyzed.

AUTHOR CONTRIBUTIONS

This work was conducted under the guidance of the author B. Aryal. All the authors have equal efforts and contribution throughout the work.

ACKNOWLEDGEMENTS

We acknowledge Sanjay Paudel, KASI, Korea, for providing a new catalogue of dwarf galaxies. We acknowledge SIMBAD, Sky View Virtual observatory, ORIGIN8.5.

CONFLICTS OF INTEREST

We declare that there are no any conflicts of interest.

EDITOR'S NOTE

This manuscript was submitted to Association of Nepali Physicists in America (ANPA) Conference 2020 for publication in the special issue of Journal of Nepal Physical Society.

REFERENCES

[1] Lelli, F.; Fraternali, F.; Verheijen M. Evolution of dwarf galaxies: a dynamical perspective. *A&A*. 2014, 563, A27.

[2] Universitat Wien, Koprolin, W. Available online: https://www.univie.ac.at/Extragalaktik/research/Dwarf.html (Accessed on 12 July 2020). Dwarf Galaxies.

[3] Andjelic, M. M. Star formation rate in Holmberg XI dwarf galaxy. *Serb. Astron. J.* 2011, N183, 71-75.

[4] Buat, V. How to measure star formation rates in galaxies. *PTA Proceedings*. 2015, vol.2, 141.

[5] James, P. A.; Shane, N. S.; Backman, J. E.; Cardwell, A. et al. The galaxy sample, Hα narrow-band observations and star formation parameters for 334 galaxies. 2004, *A&A*, 414 (1), 23-43.

[6] Kennicutt, C. R.; Lee, J. C.; Funes, G. J.; Sakai, S.; Akiyama, S. An Hα imaging survey of

galaxies in the local 11 Mpc volume. *The Astrophysical Journal Supplement Series*. 2008, 178(2), 247-279.

[7] Lee, J. C.; Gil de Paz, A.; Tremonti, C.; Kennicutt et al. Comparison of Hα and UV star formation rates in the local volume: systematic discrepancies for dwarf galaxies. *ApJ*. 2009, 706, 599.

[8] Salim, S.; Rich, R. M.; Charlot, S.; Brinchmann, J. et al. UV star formation rates in the local universe. *The Astrophysical Journal Supplement Series*. 2007, 173(2), 267-292.

[9] Cooper, M.C.; Tremonti, C.A.; Newman, J.A.; Zabludoff, A.I. The role of environment in the mass–metallicity relation. *Monthly Notices of the Royal Astronomical Society*. 2008, 390 (1), 245–256.

[10] Chhatkuli, D.N.; Paudel, S.; Aryal, B. A. Spectroscopic study of the Low Redshift Dwarf Galaxy SDSS J134326.99+431118.7 to Calculate Star Formation Rate. *BIBECHANA*. 2021, 18(1), 113-120.

[11] Paudel, S; Smith, R.; Yoon, S.J. et al. A catalog of merging dwarf galaxies in the local universe. *The Astrophysical Journal Supplement Series*. 2018, 237, 36 (20pp).

[12] Kennicutt, R. C. Star Formation in galaxies along the Hubble sequence. *Annual review of Astronomy and Astrophysics*. 1998, 36, 189-232.

[13] Marino, R. A. et al. The O_3N_2 and N_2 abundance indicators revisited: improved calibrations based on CALIFA and Te-based literature data. *Astronomy and Astrophysics*. 2013, 559, 114.

[14] Dessauges-Zavadsky, M.; Pindao, M.; Maeder, A.; Kunth, D. Classification of emission-line gal. *Vizier Online Data Catalog (J/A+A).* 2000, 355, 89.

[15] Bergvall, N. Star forming dwarf galaxies. 2011, arXiv:1105.2055v1.

[16] Lee, J. C.; Kennicutt, R.C.; Funes, S.J.J.G.; Sakai, S.; Akiyama, S. Dwarf Galaxy Starburst Statistics in the Local Volume. *The Astrophysical Journal*. 2009, 692, 1305– 1320.

[17] Sprayberry, D. *International Astronomical Union /Union Astronomique Internationale*. 1996, vol. 171, Springer, Dordrecht.

[18] Impey, C.; Bothun, G. Low surface brightness galaxies. *Annu. Rev. Astron. Astrophys*. 1997, 35, 267-307.

[19] Lelli, F.; Fraternali, F.; Sancisi, R. *A&A*. 2010, 51.

[20] Swinburne University, COSMOS. Available online: https://astronomy.swin.edu.au/cosmos/L/Low+Surface+Brightness+Galaxy (Assessed on June 2020). Low surface brightness galaxies.